Molecular Vision 2014; 20:285-300 <http://www.molvis.org/molvis/v20/285>
Received 27 September 2013 | Accepted 11 March 2014 | Published 14 March 2014

Multiple A2E treatments lead to melanization of rod outer segment–challenged ARPE-19 cells

Eugenia Poliakov,[1] Natalya V. Strunnikova,[2] Jian-kang Jiang,[3] Bianca Martinez,[1] Toral Parikh,[1] Aparna Lakkaraju,[4] Craig Thomas,[3] Brian P. Brooks,[2] T. Michael Redmond[1]

(The first two authors contributed equally to this work.)

[1]Laboratory of Retinal Cell and Molecular Biology, NEI, NIH, Bethesda, MD; [2]Ophthalmic Genetics and Visual Function Branch, NEI, NIH, Bethesda, MD; [3]NIH Chemical Genomics Center, National Center for Advancing Translational Sciences, NIH, Rockville, MD; [4]Department of Ophthalmology and Visual Sciences, School of Medicine and Public Health, University of Wisconsin-Madison, Madison, WI

Purpose: Daily phagocytosis of outer segments (OSs) and retinoid recycling by the RPE lead to the accumulation of storage bodies in the RPE containing autofluorescent lipofuscin, which consists of lipids and bisretinoids such as A2E and its oxidation products. Accumulation of A2E and its oxidation products is implicated in the pathogenesis of several retinal degenerative diseases. However, A2E accumulates in the RPE during normal aging. In this study, we used a cell model to determine the homeostatic mechanisms of RPE cells in response to A2E accumulation.
Methods: To distinguish between pathologic and normal responses of the RPE to A2E accumulation, we treated established ARPE-19 cells (cultured for 3 weeks after reaching confluence) with low micromolar amounts of A2E for several weeks. We compared the lysosomal function, lysosomal pH, degree of OS digestion, and melanization of the treated cells to untreated control cells in response to a challenge of purified rod OSs (ROSs). A2E was analyzed with high-performance liquid chromatography (HPLC); and A2E and melanin were identified with mass spectrometry.
Results: We found that post-confluent ARPE-19 cells took up and accumulated A2E under dim light conditions. Spectral analysis of the HPLC separations and mass spectrometry showed that A2E-fed cells contained A2E and oxidized A2E (furan-A2E). A2E accumulation led to a modest increase (up to 0.25 unit) in lysosomal pH in these cells. The specific activity of cathepsin D and lysosomal acid phosphatase was reduced in the A2E-treated cells, but ROS degradation was not impaired. We found that, upon challenge with ROSs, melanin pigment was induced in the lysosomal fraction of the A2E-treated ARPE-19 cells. Thus, the ARPE-19 cells responded to the A2E treatment and ROS challenge by producing a melanin-containing lysosome fraction. We speculate that this prevents them from becoming impaired in OS processing.
Conclusions: We used a modified ARPE-19 cell model in which melanization was elicited as a response to chronic accumulation of A2E. We found that although A2E treatment led, as has been previously reported, to modest lysosomal alkalinization and lysosomal impairment of ARPE-19 cells, a potential homeostatic mechanism may involve production of a special type of lysosomes containing melanin.

Incomplete degradation of outer segments (OSs) by the RPE leads to the accumulation of storage bodies containing autofluorescent lipofuscin. Lipofuscin consists of a mixture of lipids, proteins, the pyridinium bisretinoid A2E and its oxidation products, and other bisretinoids. A2E is a condensation product of two molecules of retinal and phosphatidylethanolamine (PE). Retinal isomers, including all-*trans* [1] and 11-*cis* [2], covalently react with the amine group of PE forming N-retinylidene-PE (NRPE), and this is transported across the photoreceptor disc membrane by ABCA4, an ATP-binding cassette transporter believed to function as an NRPE flippase. If the reverse reaction does not occur, releasing retinal for reduction to retinol, adding a second retinal molecule produces N-retinylidene-N-retinylphosphatidylethanolamine (A2PE), the precursor of A2E; finally, the phospholipid moiety of A2PE is removed by phospholipase D to form A2E, a reaction that occurs in the lysosomes of the RPE [3]. A2E and its products, as significant components of RPE lipofuscin, are implicated in the pathogenesis of several retinal degeneration diseases such as Best vitelliform macular dystrophy (VMD) [4], Stargardt disease [5], Stargardt-like macular dystrophy (STGD3) [6], and age-related macular degeneration (AMD). Macular dystrophies are the leading cause of visual impairment leading to irreversible blindness in the developed world [7-9]. Loss of function mutations in the *ABCA4* transporter gene causes recessive Stargardt disease. Accumulation of lipofuscin in the RPE is an important feature of Stargardt disease and usually precedes loss of vision in patients [5,10]. The mouse model of Stargardt disease

Correspondence to: T. Michael Redmond, NEI-LRCMB, NIH, Bldg 6, Rm 117A, 6 Center Drive MSC 0608, Bethesda, MD 20892-0608; Phone: (301) 496-0439; FAX: (301) 402-1883; email: redmondd@helix.nih.gov

(*Abca4*$^{-/-}$) recapitulates some features of the human phenotype, especially in the accumulation of lipofuscin pigment in the RPE, including A2E and its precursor A2PE-H_2 [11,12]. Though described in the original *Abca4*$^{-/-}$ mouse phenotype [12], effects such as delayed dark adaptation and delay in clearance of all-*trans*-retinal from the outer segments have recently been questioned, with faster rod recovery seen in *Abca4*$^{-/-}$ [13], and no delay in retinal clearance [14], compared to wild-type. These aspects have yet to be resolved.

How A2E accumulation affects RPE function is likely multifactorial [15-17], such as mediating blue light–induced damage [18] and causing lysosomal dysfunction [19]. A2E at 5 µM causes complete lysosomal membrane disintegration after 60 min, and a striking drop in the latency of the lysosomes is observed at concentrations above 2 µM [19]. Accumulation of A2E is thought to affect lysosomal pH and proteolytic function, including their ability to degrade and process the OSs [16,20]. Treatment of the ARPE-19 cell line with low levels of A2E for a longer period (3 weeks), to recreate the in vivo situation in *Abca4* $^{-/-}$ mice, increased the pH level in the lysosomes [21] that could be manipulated back to normal in compromised cells using cell-permeable analogs of cAMP [21]. Furthermore, A2E accumulation in the RPE causes mitochondrial dysfunction and renders the RPE more susceptible to oxidative stress and blue-light damage [18,22]. In contrast to the view that A2E plays a central role in AMD, recent mass spectrometric data suggested that A2E is not correlated with human macular lipofuscin [23,24]. To counter the documented adverse effects of A2E, the RPE must possess robust mechanisms to cope with a lifetime of A2E accumulation. RPE melanin has been proposed to exert a protective effect against A2E-mediated cell damage. For example, exogenous calf or human melanin added to A2E-loaded RPE cells was protective against photooxidation of A2E and blue-light damage [25]. Additionally, intact human RPE melanosomes protect bovine non-pigmented RPE cells from photosensitized and iron-mediated oxidation [26].

In view of these not completely concordant findings on the effects of A2E on RPE function, we want to better elucidate the homeostatic mechanisms of RPE cells in response to A2E accumulation. We demonstrate here that even though chronic low-level administration of A2E leads to changes in lysosomal pH and impairment of lysosomal function, normal post-confluent ARPE-19 cells respond by ramping up production of "melanized lysosomes."

METHODS

A2E synthesis: A2E synthesis followed Parish et al.'s method [27]. Briefly, ethanolamine (19 mg/352 µmol), all-*trans*-retinal (200 mg/704 µmol), and glacial acetic acid (19 µl/155 µmol) were incubated in ethanol (3 ml) at ambient temperature for 2 days in the dark. The mixture was concentrated in vacuo and purified (3X) with silica gel column chromatography using a gradient elution from 5:95 methanol:dichloromethane to 20:80 methanol:dichloromethane to give pure A2E, which was verified with nuclear magnetic resonance (NMR) spectroscopy. Approximately 50 mM A2E in ethanol was stored in aliquots in the dark at −80 °C under argon. 35 mg of A2E were diluted in 5 ml of dimethyl sulfoxide (DMSO) and aliquoted under red light in brown vials under argon (150 µl each vial), which provided a 10 mM stock solution for further dilutions. ARPE-19 cells grown on glass slides were fed with a sample of each new batch of A2E and checked with fluorescence microscopy to demonstrate comparable A2E accumulation in the cells before they were used on plates or flasks.

Cell culture and A2E treatment: ARPE-19 human RPE cells were grown to confluence, plated on 96-well, six-well plates or T75 flasks, and then maintained for 3 weeks before use in all experiments. The ARPE-19 cell batch used was validated by the ATCC Cell Line Authentication Service (Promega, Madison, WI) using short tandem repeat analysis plus the Amelogenin gender determining locus (Appendix 1). The batch was a perfect match for the ATCC human cell line CRL-2302 (ARPE-19). Stock A2E solution (10 mM in DMSO) was diluted to a final concentration of 20 nM to 10 µM in prewarmed Dulbecco's modified Eagle medium (high glucose; DMEM)/10% fetal bovine serum (FBS), 1% antibiotic-antimycotic solution (Invitrogen, Grand Island, NY) and added to the plates, as specified. Manipulations involving A2E (and vehicle) addition, and all medium changes and feedings were conducted under dim (60–65 lux) yellow (589 nm) light. Two paradigms were used to study the effect of A2E on ARPE-19 cells—single feeding and multiple feeding. For the single A2E feeding procedure, cells were fed once for 9 h with A2E (20 nM to 10 µM) and collected the next day. For long-term (chronic exposure), cells were treated overnight for 9 h four to five times over the course of treatment (3 weeks). Media were changed to the standard culture media following each treatment. Cells were evaluated for the integrity of A2E in the cells with high-performance liquid chromatography (HPLC) analysis following multiple feeding with 20 nM to 10 µM A2E. A2E in lysosomal fractions was measured spectrofluorimetrically as previously described EnVision 2104 Multilabel Reader (PerkinElmer, Waltham,

MA) fluorescein isothiocyanate (FITC) filters (excitation 485 nm, band width 14 nm/emission 535, band width 25 nm) [15].

Rod outer segment feeding of cells: Bovine rod outer segments (ROSs) were purified with discontinuous density gradient centrifugation as described originally by Papermaster and Dreyer [28] and modified by Schertler and Hargrave [29]. In brief, vigorously shake 200 bovine retinas in 180 ml sucrose buffer (45% sucrose in buffer A: 100 mM potassium phosphate, pH 7.0, containing 1 mM $MgCl_2$, 0.5 mM DTT, and 0.1 mM EDTA). This is followed by centrifugation (3,000 ×g 5 min, 4 °C) to obtain a crude ROS fraction. Filter the supernatant through gauze and dilute 1:1 with buffer A. This preparation is again centrifuged for 7 min at 4,400 ×g. Each pellet is resuspended in 1 ml of sucrose in buffer A of density 1.105. The ROS are purified by discontinuous density gradient centrifugation (18 ml of sucrose in buffer A of density 1.135, then 17 ml of sucrose in buffer A of density 1.115, and crude ROS layered on the top). The tubes are centrifuged in a Beckman (Brea, CA) SW 28 rotor for 1 h at 27,000 ×g and 4 °C without the brake. ROS is collected as slightly orange band at the 1.115 -1.135 interface. This ROS suspension is diluted 1:1 with buffer A and harvested by centrifugation at 39,000 ×g and 4 °C. Pellets are stored at -80 °C until use. For feeding cells, the ROS were solubilized in 100 mM bicarbonate buffer with 10% sucrose (pH = 8.5), counted in a hemocytometer, and administered at a concentration of 1×10^7 ROS/ml. ROS were added for 6 h followed by an 18-h chase with fresh media. Then the ARPE-19 cells were collected, and the lysosomes were immediately isolated.

High-performance liquid chromatography analysis of A2E: Pelleted RPE cells (225 cm^2 flask) were washed once with 1 ml phosphate-buffered saline (PBS ; 1X, 137 mM NaCl, 2.7mM KCl, 10 mM $NaHPO_4$, 1.8 mM KH_2PO_4, pH 7.4), homogenized in 975 µl H_2O and 2.5 ml methanol-glacial acetic acid (98:2), and then 1.125 ml chloroform was added to get a single phase solution. The solution was thoroughly mixed and centrifuged for 5 min at 16,000 ×g to pellet proteins. Then 1.225 ml of chloroform and 1.225 ml of H_2O were added, the tube was mixed for 1 min to separate into two phases, and the lower organic phase containing A2E was collected. A2E was analyzed with reverse phase HPLC, as previously described [15]. Briefly, samples were injected on a C30 YMC 4.6 × 150 mm column (YMC America, Allentown, PA) and eluted with a gradient of methanol in water (84–98% methanol + 0.1% trifluoroacetic acid (TFA), gradient 84% to 96% in 10 min and 96% to 98% in another 10 min, 0.8 ml/min; an Agilent 1200 HPLC system equipped with a diode-array detector was used, and the data were analyzed with ChemStation32 software (Agilent Technologies, New Castle, DE). Specific wavelength detection was used for monitoring A2E (430 nm), and A2E and furan-A2E absorption spectra were extracted from the chromatograms. The quantities of A2E in cultured RPE were determined from the integrated peak intensities.

Measurement of the effect of A2E on lysosomal pH: LysoSensor Yellow-Blue DND-160, (Invitrogen; 1 µM: add 3 µl of 1 mM LysoSensor Yellow-Blue DND-160 concentrate to 3 ml of medium) and LysoTracker Red DND 99, (Invitrogen; 50 nM:1 µl of LysoTracker to 5 ml of media) solutions were prepared and added to the cells. LysoSensor Yellow/Blue DND-160 colocalized with the LysoTracker Red dye in small vesicles, with a distribution consistent with lysosomal origin. The pH was measured using a high throughput screening (HTS) protocol to maximize the output and minimize the variation. ARPE-19 cells in 96-well plates were loaded for 5 min at 23 °C with 1 µM LysoSensor, followed by 15 min for internalization, and produced stable and reproducible results.

Fluorescence (ex 360 nm/em >527 nm) of LysoSensor DND-160 was measured for 20 msec, every 30 s, to minimize bleaching. The change in fluorescence at 528 nm from the control cells was converted to Δ pH by calibration with KCl buffered to pH 4.4 to 6.0 in the presence of 10 µM of the H^+/Na^+ ionophore monensin and 10 µM of the H^+/K^+ ionophore nigericin dissolved in 20 mM 2-(N-morpholino) ethane sulfonic acid (MES), 145 mM KCl, 10 mM glucose, and 1 mM $MgCl_2$ adjusted to pH 4.4 to 6.0 with HCl/NaOH. The vH^+ATPase inhibitor bafilomycin A1 (BfA) and chloroquine (CQ) were used as positive controls for the lysosomal change in the control ARPE-19 cells. The cells were treated in DMEM + 1% FBS for 3–5 h with 50 nM or 500 nM BfA (from 50 µM stock solution in DMSO), or 1 µM or 100 µM CQ. After the treatments, the cells were washed with 1X Hank's Balanced Salt Solution (HBSS), and LysoSensor was added in HBSS for 30 min at 37 °C. Plates were read on a plate reader at ex 360/em 528, with a bottom sensitivity of 50.

3-(4,5-dimethylthiazol-2-yl)-2,5-diphenyltetrazolium bromide cell viability assay: The ARPE-19 cells were seeded in 96-well collagen-coated microculture plates and treated with varying concentrations of hydroquinone (HQ; 50–500 µM) for 16 h, followed by a 24-h recovery period in 1% FBS in DMEM media [30]. At the 40-h point, the number of viable cells was then determined by adding 3-(4,5-dimethylthiazol-2-yl)-2,5-diphenyltetrazolium bromide (MTT) for 4 h following the manufacturer's instructions (Cell Proliferation Kit I; Roche Molecular Biochemicals, Indianapolis, IN).

Immunofluorescence microscopy: The ARPE-19 cells were grown on slides, treated with 10 µM A2E, LysoTracker Red DND 99 (50 nM), and 4',6-diamidino-2-phenylindole

dihydrochloride (DAPI; 1:1,000). The cells were visualized using an Olympus FLUOVIEW FV1000 confocal microscope (Olympus America, Melville, NY) with excitation/emission wavelengths 405 nm/em 461 nm (DAPI), ex 488 nm/ em 520 nm (A2E autofluorescence), and ex 559 nm/em 603 nm (LysoTracker Red) with laser power at 10% and 60× magnification.

Isolation and immunoblotting of lysosomal fractions: Lysosomal fractions from eight flasks (175 cm^2) of ARPE-19 cells in each group were prepared by gradient ultracentrifugation using a Lysosome Isolation Kit (Sigma, St. Louis, MO), following the manufacturer's recommendations. Samples were prepared for sodium dodecyl sulfate–polyacrylamide gel electrophoresis (SDS–PAGE). Denatured samples were separated on 10% BisTris NuPage (Life Technologies, Grand Island, NY) gels and electrotransferred to nitrocellulose membranes. Blots were probed with antibodies with standard procedures and developed in color substrate BCIP/NBT Phosphatase substrate (KPL, Gaithersburg, MD). The following antibodies were used: antilysosomal-associated membrane protein 1 (LAMP1; Cell Signaling, Danvers, MA; C54H11) rabbit monoclonal antibody, premelanosome protein 17 (PMEL17) rabbit polyclonal antibody (Santa Cruz, Dallas, TX; SC-33590), mouse monoclonal antibody against tyrosinase-related protein 1 (TYRP1; Santa Cruz, SC-166857), and mouse monoclonal antibody against tyrosinase (TYR; Santa Cruz, SC-20035). The secondary antibody used was alkaline phosphatase-conjugated goat anti-rabbit immunoglobulin G (IgG) or alkaline phosphatase-conjugated goat anti-mouse IgG (1:10,000; EMD-Millipore, Billerica, MA), as appropriate.

Acid phosphatase and cathepsin D activity in lysosomes: Lysosomal fractions (40 µl) were incubated on enzyme-linked immunosorbent assay (ELISA) plates with p-nitrophenyl phosphate (PNPP) substrate solution (50 µl; one tablet dissolved in 2.5 ml of 0.1 M citrate buffer, pH 4.8) for 20 min, and the reaction was quenched with 50 µl of 0.5 N NaOH. Absorbance was read at 405 nm. Acid phosphatase (potato (6 units/mg); Sigma) was used for the calibration curve. Cathepsin D activity in lysosomal fractions was measured with the Sensolyte 390 Cathepsin D Assay Kit (Anaspec, Fremont, CA) according to the manufacturer's recommendations. Lysosomal fractions (10 µl) were mixed with 40 µl of assay buffer and 50 µl of substrate solution in ELISA Optiplates (PerkinElmer) and incubated for 20 min under yellow light. Fluorescence was read at ex 355 nm/em 400 nm.

Spectroscopic and matrix-assisted laser desorption-ionization time-of-flight analysis of melanin and A2E in lysosomal fractions: The absorption spectra of the lysosomal fractions were measured from 300 to 720 nm in an ultraviolet (UV)-visible spectrophotometer (Shimadzu UV-2501 PC, Columbia, MD). The λ_{max} of A2E is approximately 439 nm [27], and that of the synthetic melanin standard is 335 nm [31]. Synthetic melanin (Sigma) was dissolved in acetonitrile (2 mg/ml) and then further diluted in acetonitrile:0.5 N KOH (1:1). A solution of 250 mM 2,5-dihydroxybenzoic acid (DHB) was prepared fresh each day in 1:1 acetonitrile:water. Melanin and DHB were mixed 1:1 and spotted on a matrix-assisted laser desorption-ionization (MALDI) plate. MALDI spectra were obtained using an ABI Sciex (Framingham, MA) Voyager DE-STR matrix-assisted laser desorption-ionization time-of-flight (MALDI-TOF) instrument in the reflective positive mode with 20,000 accelerating voltage, 64.2% grid voltage, 2775 laser intensity, 125 nsec delay, and range m/z 150–1000. Lysosomal fractions mixed with DHB in a 1:1 ratio with a laser setting of 1950 gave clean spectra of A2E (m/z 592 and minor oxidation product m/z 608). Acetonitrile extracts of lysosomal fractions at a laser setting of 2775 demonstrated a pattern of peaks similar to synthetic melanin.

RESULTS

Uptake of A2E by differentiated ARPE-19 cells: A2E and its oxidation products are deposited in the RPE during normal aging. In some disease states, it is proposed, based on in vitro experiments, that accumulation of A2E can impair the lysosomal and mitochondrial function of RPE cells ultimately leading to RPE apoptosis and vision loss. As a model of A2E accumulation in RPE cells, 3-week post-confluent ARPE-19 cells were loaded with various concentrations of A2E (20 nM, 100 nM, 1 µM, 10 µM), using a single dose or multiple doses [5]. Following extraction from the harvested cells, A2E and its oxidation products were separated with reverse phase HPLC and quantified using an A2E calibration curve (the area of the A2E (all isomers) peak (at approximately 430 nm) was linear in the range from 25 pmol to 125 nmol; data not shown). According to the absorption spectra, the peaks at 10.4–10.9 min were consistent with A2E (insets). Uptake of A2E by ARPE-19 cells was linear for the 100 nM to 10 µM range in the single and multiple treatment experiments (Table 1 and Appendix 2). HPLC analysis of A2E extracted from cells after multiple or single feedings (100 nM to 10 µM) confirmed that A2E was detected in cell extracts showing similar oxidation patterns (Figure 1A,B). The peaks at 7.9 min were identified by their absorption spectra as furan-A2E (blue shift of approximately 40 nm in early λ_{max} (inset [32]). This identification is consistent with the occurrence of the mass of m/z 608 observed with mass spectrometry. We did not detect A2E accumulation when it was fed at the 20 nM

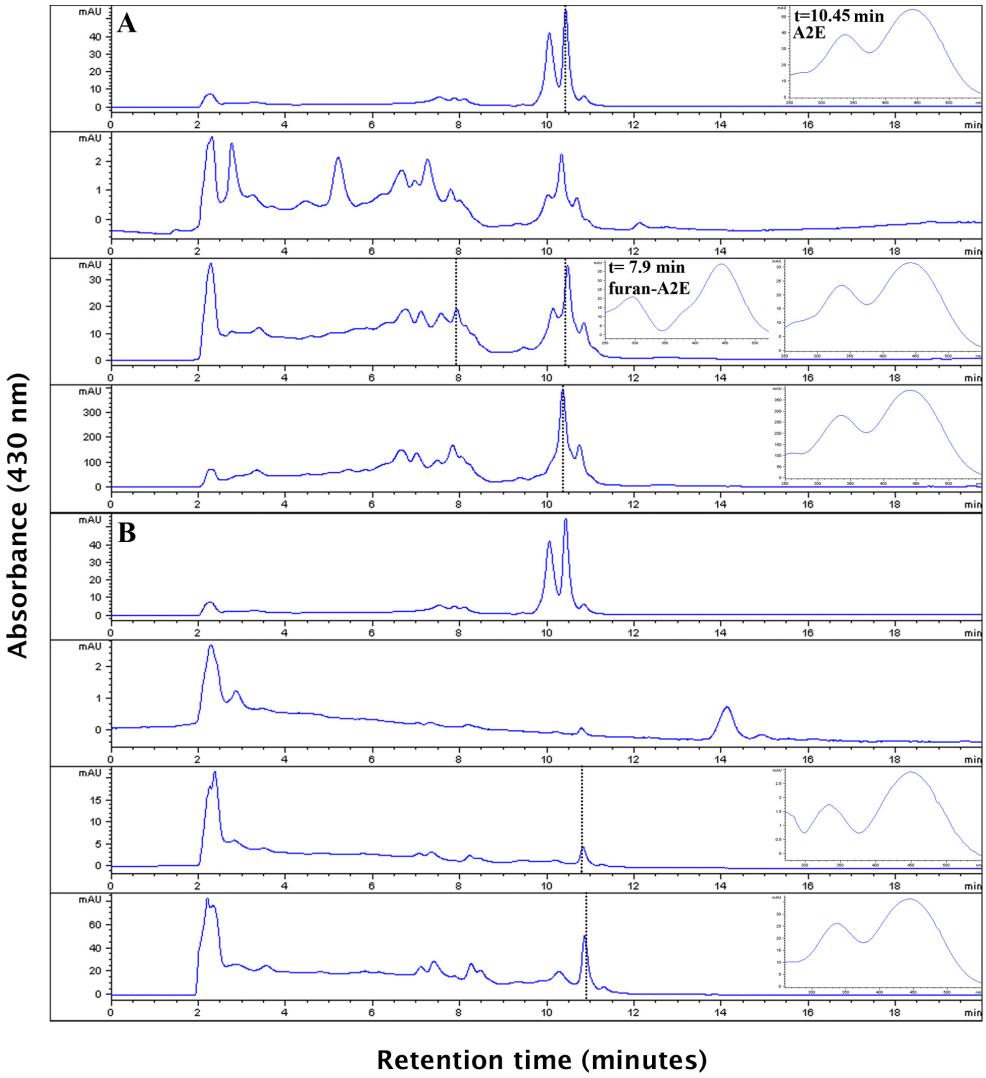

Figure 1. Accumulation of A2E in ARPE-19 cells. **A**: Reverse phase high-performance liquid chromatography (HPLC) of A2E: from top to bottom, A2E standard, extracts of cells multiple-fed 100 nM, 1 µM, and 10 µM A2E, respectively, delivered in dimethyl sulfoxide (DMSO). The absorption spectra (250 to 550 nm) of the A2E peak (10.4–10.9 min) are shown (insets) for the standard and 1 µM and 10 µM chromatogram. An absorption spectrum (250–520 nm) of the furan-A2E peak (7.9 min) is also shown. Dotted lines indicate the peaks whose spectra were scanned. **B**: Reverse phase HPLC of A2E: from top to bottom, A2E standard, extracts of cells single-fed 100 nM, 1 µM, and 10 µM A2E, respectively, delivered in DMSO. The absorption spectra (250 to 550 nm) of the A2E peak (10.4–10.9 min) are shown (insets) for the 1 µM and 10 µM chromatograms. Dotted lines indicate the peaks whose spectra were scanned. Results shown are representative of two separate experiments.

concentration at either single or multiple feedings (data not shown).

A2E is stored in and alkalinizes lysosomes in single and multiple feeding experiments: When post-confluent ARPE-19 cultures were fed with 10 µM A2E and the cells were visualized next day, A2E fluorescence (Figure 2A) and LysoTracker fluorescence (Figure 2C) were colocalized (Figure 2D). This colocalization varied in intensity, depending on the level of A2E accumulation by individual cells. Feeding with lower concentrations of A2E did not produce a reliable fluorescent signal on microscopy. To confirm lysosomal localization of A2E, ARPE-19 cells were fed five times during 3 weeks with 1 µM A2E in DMSO or DMSO vehicle alone. The lysosomal fraction from these cells was isolated, and A2E fluorescence was compared (Figure 3A). A2E fluorescence was not seen in the control cells while A2E fluorescence in the fractions of A2E-treated cells coincided with lysosomal marker LAMP1 expression in these fractions (Figure 3B), indicating that the lysosomes in the A2E-treated cells actually contained A2E. Because multiple feedings with A2E over time might more closely approximate in vivo physiology than a single feeding, and because we demonstrated robust colocalization of A2E to lysosomes using more than one technique, we

Table 1. Quantification of A2E extracted from ARPE-19 cells

A2E extracted (ng/10^5cells)					
A2E multiple treatment (5 times)			A2E single treatment (1 time)		
100 nM	1 µM	10 µM	100 nM	1 µM	10 µM
2.4	39.4	425.6	0.5	8.5	83.6

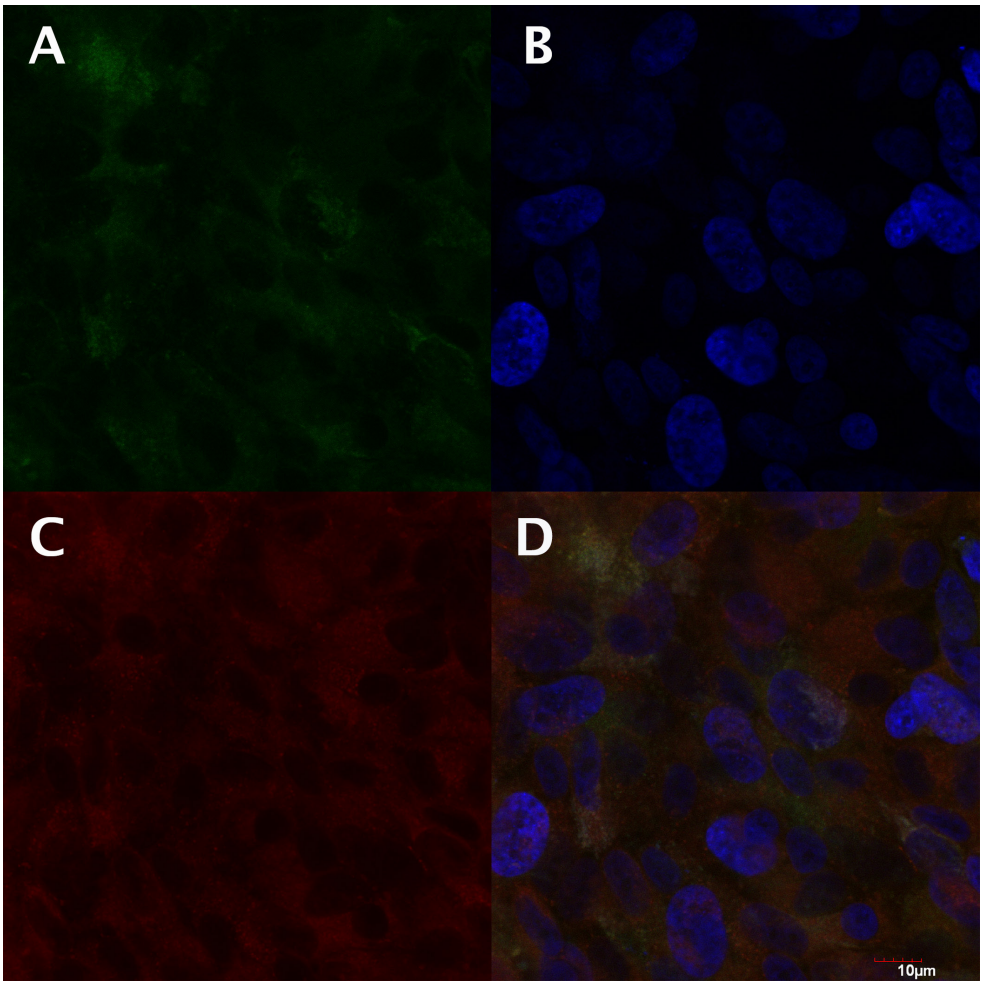

Figure 2. Partial colocalization of A2E and LysoTracker fluorescence in A2E-fed ARPE-19 cells (60× magnification). **A**: A2E autofluorescence; **B**: 4',6-diamidino-2-phenylindole dihydrochloride (DAPI); **C**: LysoTracker Red DND 99; and **D**: merged. Confocal microscopy was performed on an Olympus FV1000 confocal microscope with detection in DAPI, green (fluorescein isothiocyanate, FITC), and red (rhodamine) channels as described. Results shown are representative of two separate experiments.

chose the multiple feeding paradigm for the remainder of our experiments.

Multiple-feeding of ARPE-19 cells with 10 µM A2E caused rapid and obvious cell death, whereas feeding with 1 µM A2E did not. To determine the viability of the cultured ARPE-19 cells treated with different concentrations of A2E, the cells were exposed to various concentrations (50–500 µM) of hydroquinone to evoke oxidative stress and were evaluated with an MTT cell viability assay at 570 nm. We found that multiple A2E treatments at 1 µM or lower concentration did not produce any more cell death in cells than in the control cells challenged with hydroquinone alone. Consistent with our qualitative observations, multiple 10 µM A2E treatments led to cell death (Figure 4).

Our next question was whether A2E would induce lysosomal alkalinization in ARPE-19 cells. To answer this question, we used the lysosomal pH indicator dye LysoSensor Yellow/Blue DND-160 calibrated with KCL buffers in the range of pH 4.4 to pH 5.6. Chloroquine (CQ) and the vH^+-ATPase inhibitor, bafilomycin-A1 (BfA), alkalinize lysosomal pH and were used as the controls [33,34]. In confluent ARPE-19 cells, adding CQ or BfA led to dose-dependent alkalinization of lysosomal pH (Figure 5A). These data are in good agreement with previously published data [35,36]. We found that the multiple feeding protocol of 20 nM to 10 µM A2E to ARPE-19 cells led to an approximate 0.05–0.25 unit pH increase in the lysosomes compared to the untreated controls (Figure 5B).

A2E accumulation leads to impaired catalytic activity of lysosomal enzymes: The activity of lysosomal enzymes has long been known to be sensitive to changes in pH [37]. We therefore measured the activity of two major lysosomal enzymes, cathepsin D and acid phosphatase, in lysosomal fractions isolated from cells with or without chronic A2E treatment and ROS challenge by quantifying fluorescent (ex 355/em 400; Figure 6A) and colorimetric reaction products (405 nm), respectively (Figure 6B). As others have previously reported, we confirmed impairment in the specific activity

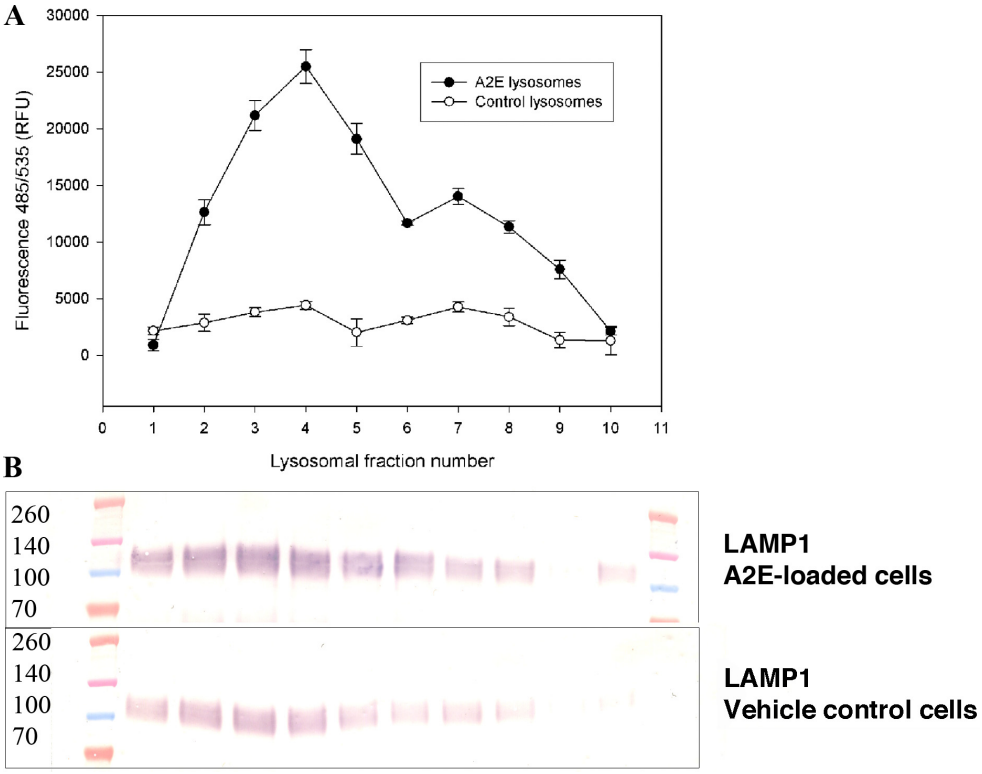

Figure 3. Presence of A2E in the lysosomal fraction of multiple 1 µM A2E-treated ARPE-19 cells compared to untreated ARPE-19 cells. **A**: A2E fluorescence (ex 485/em 535) was measured in lysosomal fractions prepared with gradient ultracentrifugation. **B**: Lysosomal-associated membrane protein 1 (LAMP1) lysosomal marker expression in immunoblots of the same fractions was probed with the LAMP1 primary antibody.

of lysosomal enzymes (activity normalized to total protein concentration). However, we also observed an increase in the total activity of the lysosomal proteins and the protein amount in the lysosomal fractions in the A2E-treated cells compared to the controls (Figure 6A,B; see also Figure 3).

Rod outer segments challenge leads to melanization of A2E-accumulating ARPE-19: Melanin protects RPE cells from oxidative stress [38] and may affect lipofuscin accumulation [39]. We found that upon challenge with ROSs (1×10^7 ROS/ml for 6 h followed by an 18-h chase with fresh media), the A2E-treated cells became pigmented and that the pigment copurified with the lysosomal fraction (Figure 7A). We found that the lysosomal fractions were positive for the presence of the lysosomal marker LAMP1 marker (not shown) and the premelanosomal marker PMEL17 (Figure 7B). Lysosomes from the A2E-treated pigmented cells contained more tyrosinase-related protein 1 (TYRP1), melanosomal 5,6-dihydroxyindole-2-carboxylic acid oxidase, than the control cells (Figure 7B). However, we did not detect TYR in these lysosomal fractions. We observed for the first time that chronic low micromolar A2E exposure and subsequent ROS challenge induced melanization of ARPE-19 cells as determined with spectroscopy, HPLC, and MALDI-TOF analysis. First, MALDI-TOF mass spectrometry of lysosomal fractions (Figure 8) demonstrated the presence of A2E (m/z 592 and a minor oxidation product of m/z 608, consistent with the identification of furan-A2E by the absorption spectrum [Figure 1A]). We did not detect these peaks in the control lysosomal fractions (data not shown). For melanin, we analyzed acetonitrile extracts of these fractions with MALDI-TOF mass spectrometry. We detected melanin degradation products [40] with masses of m/z 441, 495, 523, 537, 551, and 565 (Appendix 3) that were also found in synthetic melanin spectra (inset in Appendix 3), but without the lower m/z peaks of 304, 329, and 332 found in the latter. In addition, by collecting the absorption spectra (range 300 to 720 nm) of the lysosomal fractions purified from the A2E-challenged cells, we demonstrated the presence of A2E (λ_{max}: approximately 439 nm) and melanin (λ_{max}: approximately 335 nm) [31] and their apparent colocalization in fractions 3 and 4 (Appendix 4). The apparent absence of the 339 nm peak of A2E in these spectra is unexplained but could be due to interaction with melanin.

Rod outer segment degradation is not impaired in melanized A2E-treated ARPE-19 cells: ROSs were added to the cells at concentration of 1×10^7 ROS/ml for 6 h followed by an 18-h chase with new media. Then cells were collected and the lysosomal fractions immediately isolated by density step gradient centrifugation. The lysosomal fractions were probed with 1D4 anti-rhodopsin monoclonal Ab. We found

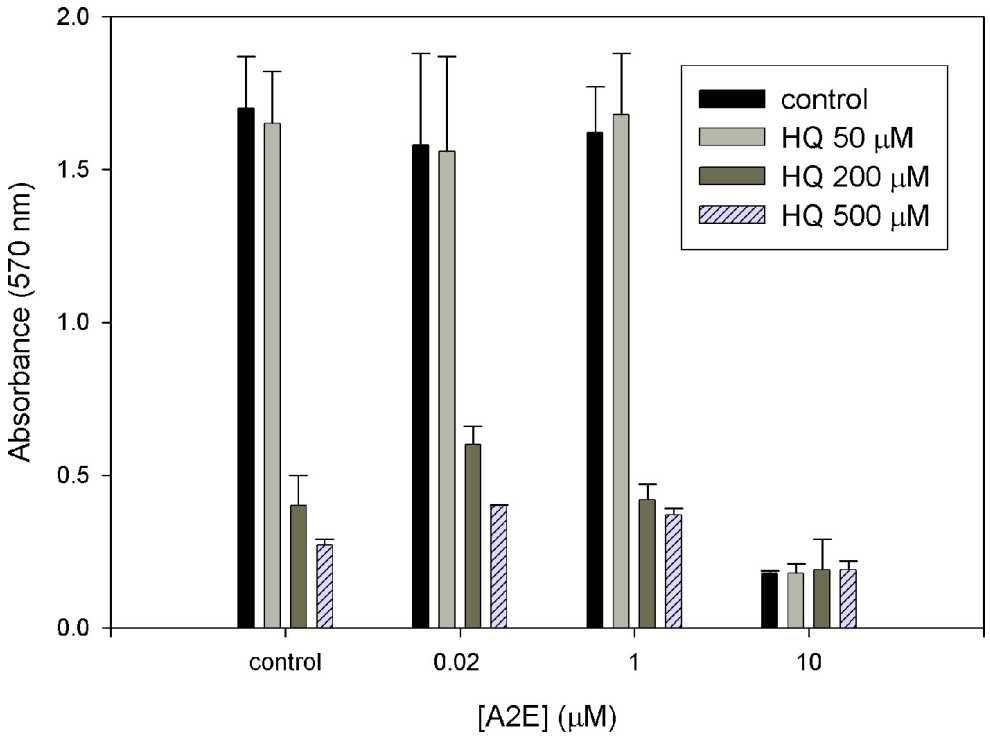

Figure 4. Sensitivity of ARPE-19 cells to hydroquinone oxidative stress in the presence of various concentrations of A2E. The viability of ARPE-19 cells treated with 50–500 μM hydroquinone (HQ) in the presence of 0, 20 nM, 1 μM, or 10 μM A2E for 16 h, followed by 24 h recovery, was measured with 3-(4,5-dimethylthiazol-2-yl)-2,5-diphenyltetrazolium bromide (MTT) cell viability assay. n = 3 for each condition.

that the amount of rhodopsin in the lysosomal fractions of the A2E-treated cells was comparable to those of the control cells. Therefore, these results suggest that ROS degradation is not impaired in A2E-treated pigmented ARPE-19 cells (Figure 9).

DISCUSSION

In this paper, we showed that even though chronic low-level administration of A2E, an important component of RPE lipofuscin, led to a small increase in lysosomal pH and modest lysosomal impairment, normal post-confluent ARPE-19 cells responded by giving rise to what we call "melanized lysosomes." To understand the chronic effects of A2E in an "aging RPE" model system, we studied compensatory mechanisms that might counteract its adverse effects. We treated post-confluent differentiated ARPE-19 cells with low doses of A2E for several weeks to determine its effect on lysosomal pH levels and ROS degradation. We found that feeding A2E-challenged cells with ROSs led to melanization of cells in parallel with clearance of the ROSs by the cells. We discuss these results in the context of the homeostatic mechanisms of RPE cells in response to the normal uptake of A2E and other bisretinoids over a lifetime.

The role that A2E plays in the pathogenesis of macular dystrophies, early onset such as Stargardt disease and late onset such as geographic atrophy (GA) in AMD, remains somewhat controversial. Massive accumulation of A2E and other lipofuscin bisretinoids is a hallmark of Stargardt disease, but the precise role A2E plays in the pathobiology of Stargardt disease is unclear though several possible mechanisms have been investigated [15-17]. Increased fundus autofluorescence (FAF; a clinical surrogate for lipofuscin/bisretinoid accumulation) in RPE-bordering GA lesions has been interpreted as supplying causality for lipofuscin/bisretinoid toxicity in these RPE cells leading to GA [41,42]. However, the pathophysiological relevance of variations in FAF has been debated [43,44]. Meanwhile, the proposed role of A2E and other bisretinoids in Stargardt disease and GA has led to the proposal of therapies for these diseases focused on reducing visual cycle flux (e.g., inhibitors of visual cycle enzymes including RPE65 and RDH5, reducing retinol delivery to the RPE) and thus reducing accumulation of bisretinoid components of lipofuscin. Clinical trials for some such compounds have been performed or are under way. Contrary to this view, Ablonczy and colleagues recently demonstrated that although A2E may accumulate in human peripheral RPE, similar to the mouse RPE as a whole, the

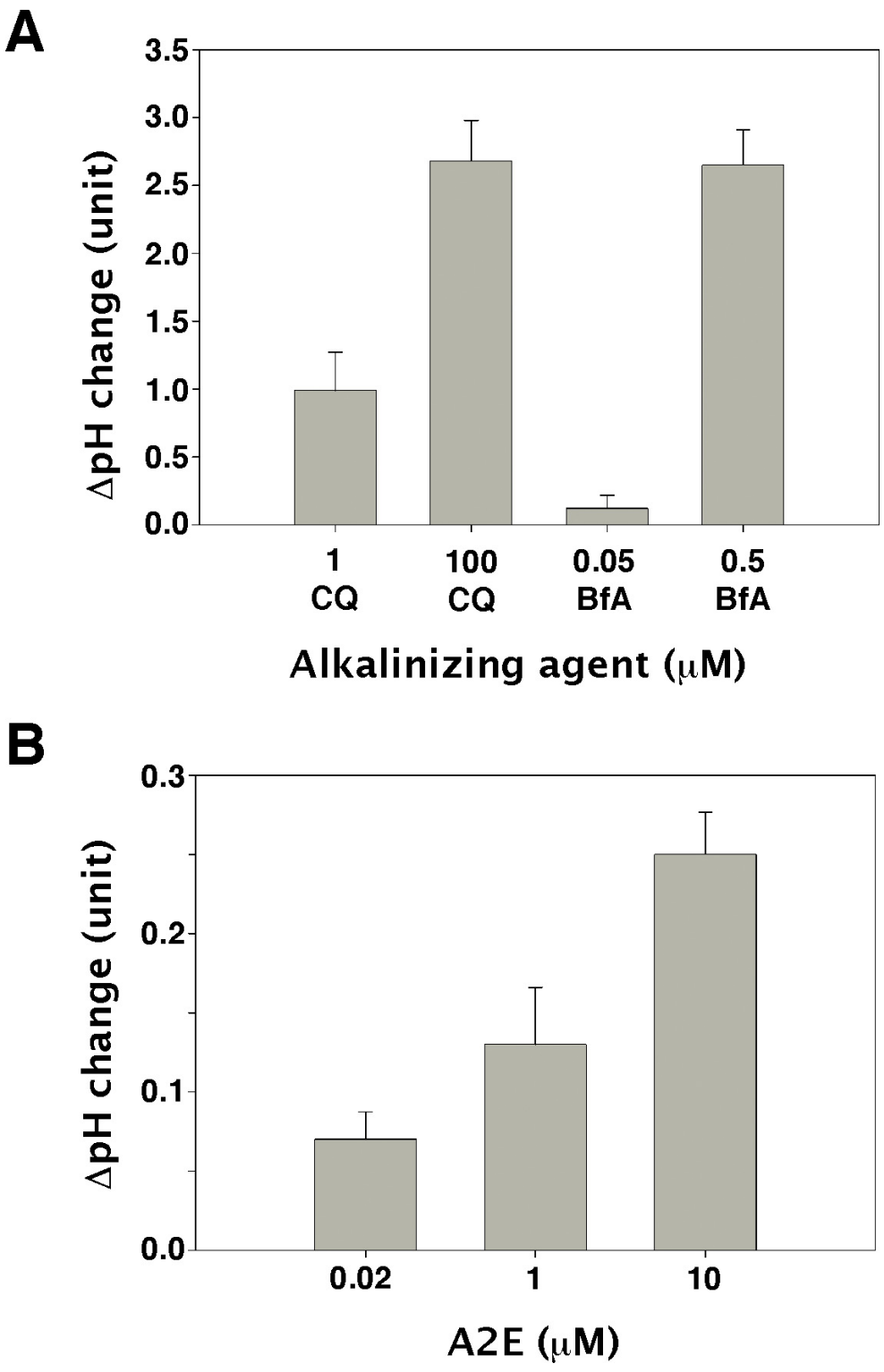

Figure 5. Alkalinization of ARPE-19 lysosomes by chronic treatment with A2E. **A**: Bafilomycin-A1 (BfA; 500 nM) and chloroquine (CQ; 1 and 100 μM) positive controls caused a large increase in lysosome pH from approximately 1 pH unit to approximately 2.6 pH units. **B**: Chronic treatment of ARPE-19 cells with A2E led to a moderate increase in lysosomal pH. Lysosomal pH was measured using LysoSensor DND160 calibrated against the control cells treated with KCl buffered at values from pH 4.4 to 6.0 in the presence of monensin and nigericin. n = 3 for each experimental condition.

accumulation does not appear to correlate with the increase in lipofuscin in the aging human macular RPE. These authors suggest that other compounds may be responsible [23,24].

In contrast to the more or less rapid, putatively toxic, accumulation of lipofuscin/bisretinoids implicated in Stargardt disease, slower physiologic accumulation occurs in normal aging of the RPE [45]. That high concentrations of

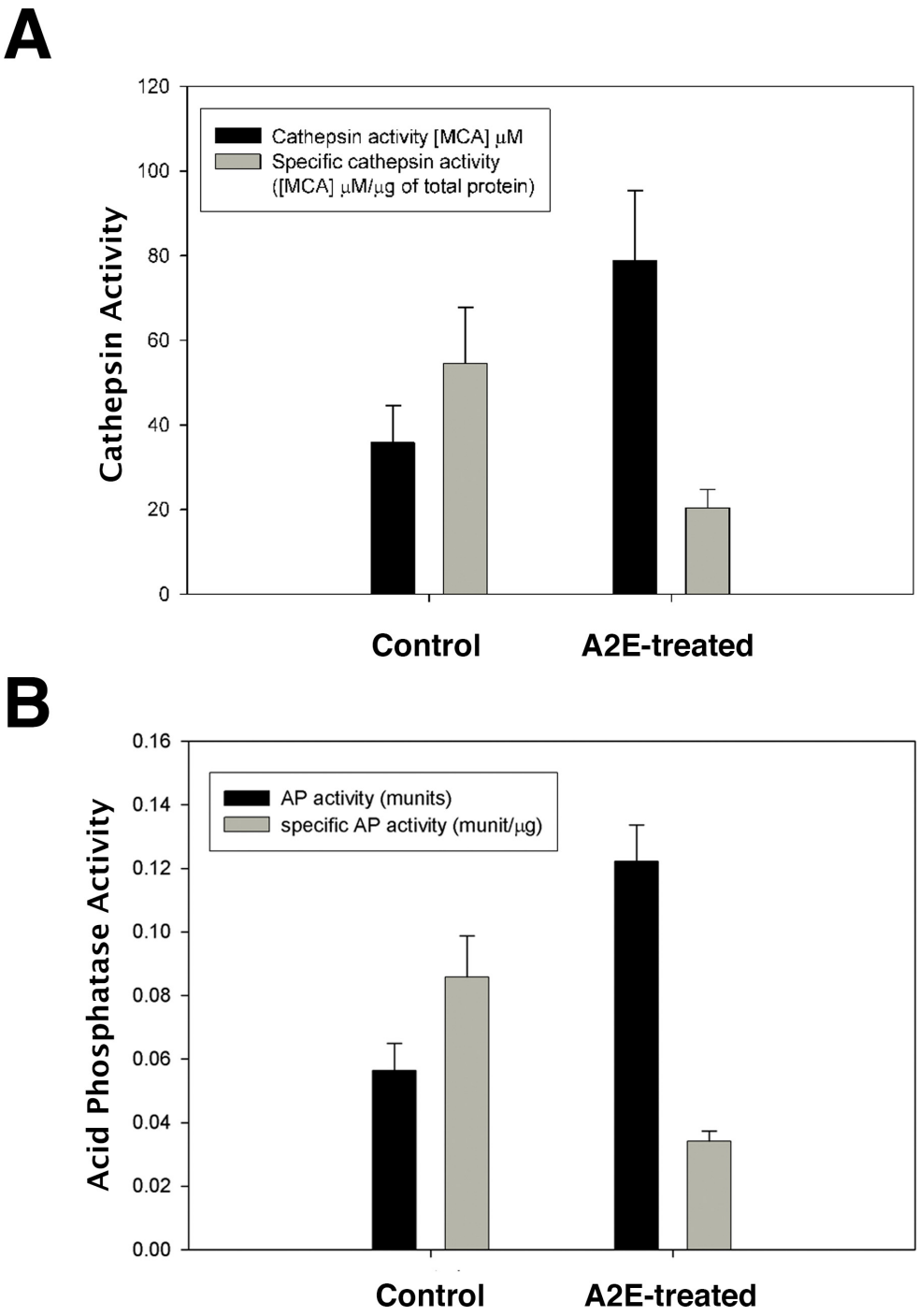

Figure 6. Lysosomal enzyme activities of A2E-treated ARPE-19 cells challenged with rod outer segments. **A**: Cathepsin D activity of the ARPE-19 lysosomal fraction prepared from control and multiple 1 µM A2E-treated cells fed with rod outer segments (ROSs). Enzyme activity was measured with the Sensolyte 390 kit (n = 4 for each experimental condition). **B**: Acid phosphatase activity of the ARPE-19 lysosomal fraction prepared from control and multiple 1 µM A2E-treated cells fed with ROSs. Enzyme activity was measured with the standard p-nitrophenyl phosphate (PNPP) assay (n = 4 for each experimental condition).

A2E, a major component of the bisretinoids of lipofuscin, transported to RPE lysosomes in vitro can inhibit lysosomal degradative function are well described in the literature [16,20]. The A2E-induced increase in the lysosomal pH and inhibition of the lysosomal proton pump [17], and slowing of cholesterol efflux from lysosomes [46], has been demonstrated. Since A2E is a quaternary amine, it cannot bind protons and thus directly affect pH [1]; however, as a cationic detergent, A2E could disrupt the integrity of lysosomal membranes [1]. A recent study demonstrated that indeed A2E has the capacity to cause leakage of lysosomal membranes, which could contribute to lysosomal pH changes [19]. In contrast, restoration of lysosomal pH in RPE cells from *Abca4*$^{-/-}$ mice led to the recovery of lysosomal function

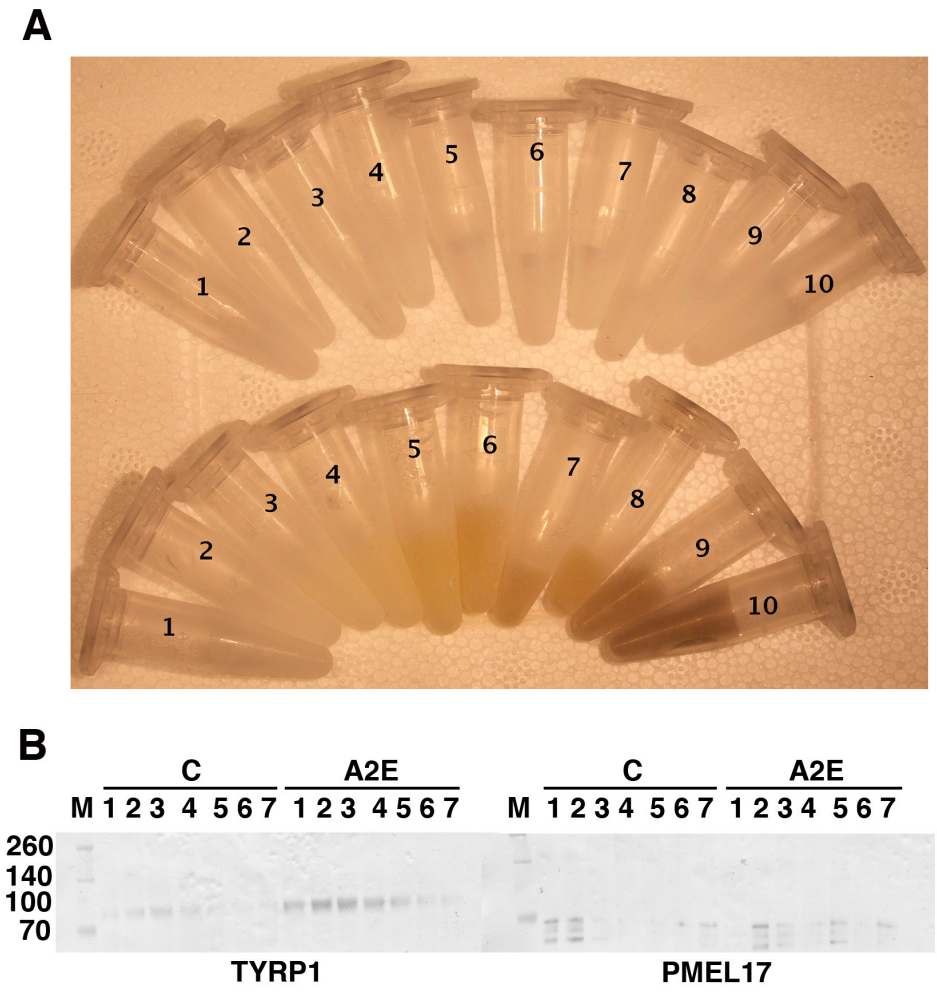

Figure 7. Melanization of A2E-treated ARPE-19 cells. **A**: Isolated lysosome preparations from the untreated control (left) and multiple 1 µM A2E-treated cells (right) show brown melanin pigment in the A2E-treated cells and not in the control cells. **B**: Increased expression of tyrosinase-related protein 1 (TYRP1) but not premelanosome protein 17 (PMEL17) was detected in immunoblots of isolated lysosomal fractions from sub-cellular fractionation of control (C) and multiple 1 µM A2E-treated (A2E)-treated ARPE-19 cells by density gradient ultracentrifugation, probed with anti-TYRP1 and anti-PMEL17 primary antibodies. Results shown are representative of three separate experiments.

[21]. The potentially toxic effects of A2E accumulation are delineated for high A2E concentrations in the mouse model of recessive Stargardt macular degeneration [47], but the degree of A2E's toxicity to RPE cells in vitro at low micromolar concentrations varies, ranging from DNA protective effects [48] to mitochondrial damage and apoptosis [49]. We believe that such a discrepancy in effects could be partially explained by the differences in the state of the cell, delivery of A2E, and variability in compensatory effects of cells. In this paper, we sought to simulate physiologic chronic low exposure of differentiated ARPE-19 cells with A2E and ROSs. Surprisingly, we found that the post-confluent differentiated ARPE-19 cells responded to A2E administration by inducing melanization and producing lysosomes containing melanin. Although most melanosomes, including those of the RPE, arise prenatally in development, some degree of processing occurs postnatally, along with loss of melanosomes due to aging [50]. Whether our correlation of melanin with lysosomes in these experiments coincides with the "melanolysosomes" described by Feeney in the aging RPE is not clear [51]. Feeney suggested that melanin in these bodies is undergoing "remodeling" and/or "degradation." In contrast, we observed apparent de novo biosynthesis of melanin. We observed the strong presence of LAMP1, PMEL17, and TYRP1 markers in our lysosomal fractions that correspond to stage II or stage III premelanasomes [52]. PMEL17 is mostly involved in eumelanin production [53]. Melanosomes are categorized as lysosome-related organelles derived from early endosomes, which also give rise to the precursors of lysosomes [54], and melanosomes have been shown to contain many lysosomal hydrolases [55]. The close functional relationship of melanosomes and lysosomes in the RPE has been addressed (for review, see

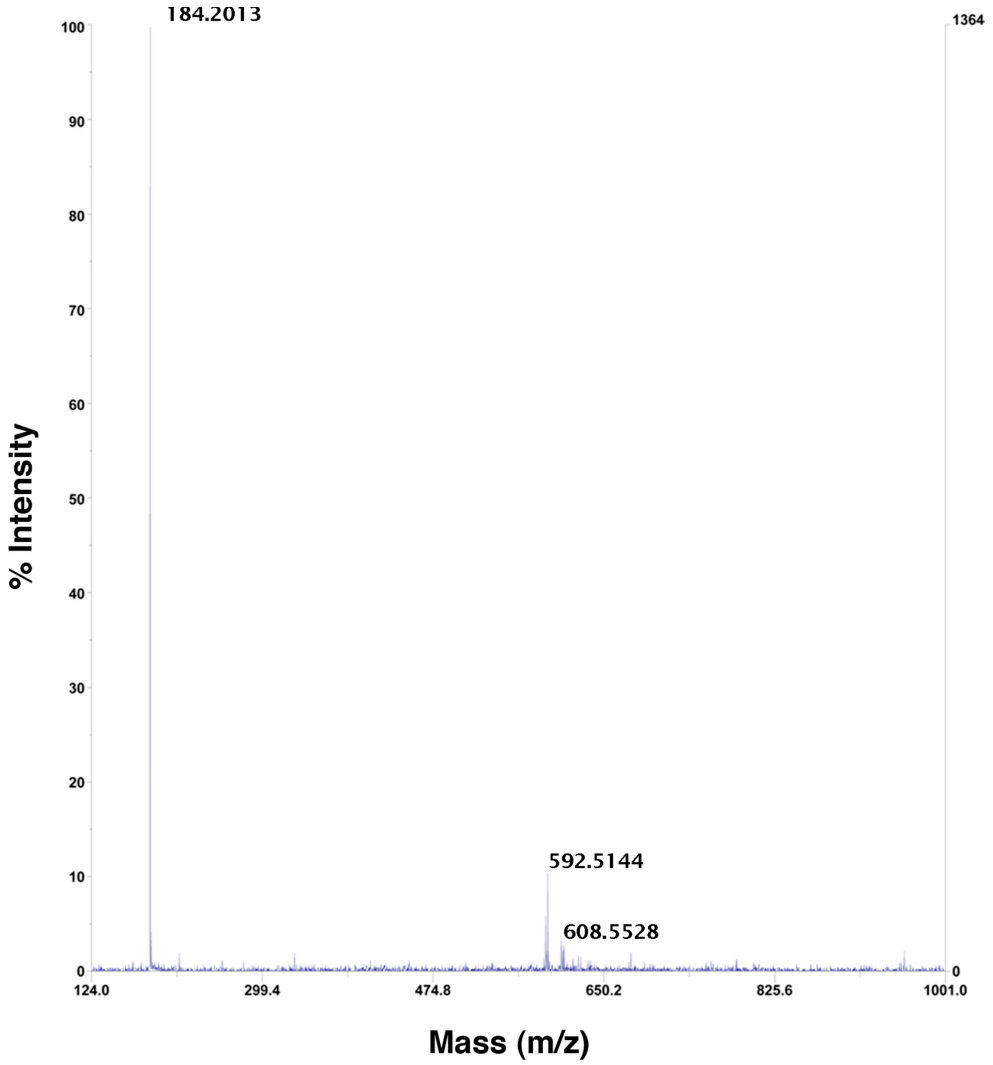

Figure 8. A2E is present in ARPE-19 lysosomal fractions. Matrix-assisted laser desorption-ionization time-of-flight (MALDI-TOF) mass spectrometric analysis of lysosomal fraction 8 (see Figure 7A) isolated from multiple 1 µM A2E-treated ARPE-19 cells show the presence of A2E (m/z 592) and a minor oxidation product (m/z 608) consistent with furan-A2E. Results shown are representative of three separate experiments.

[56]). Quinolines such as chloroquine that cause lysosomal swelling [33] also affect RPE melanosomes [57]. Melanoregulin (MREG), a protein that regulates pigmentation, also modulates lysosome function and lysosome maturation in the RPE [58]. Melanin-containing cells accumulate less lipofuscin than albino or poorly pigmented cells [39]. This may be due to melanin's ability to scavenge reactive oxygen species [25]. The melanized cells in our experiments degraded OSs as well as ARPE-19 cells that had not been treated with A2E.

We confirmed here that a major effect of chronic low micromolar A2E exposure is alkalinization of lysosomes

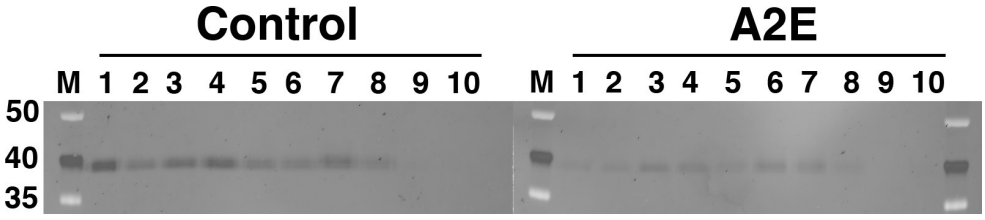

Figure 9. Degradation of rod outer segments is not impaired in melanized 1 µM A2E-treated ARPE-19 cells. Immunoblots of lysosomal fractions of melanized multiple 1 µM A2E-treated ARPE-19 cells challenged with rod outer segments (ROSs) were probed with anti-rhodopsin D4 monoclonal antibody and Cy3-conjugated goat anti-mouse ECplex fluorescent antibody (1:2,500, Amersham Biosciences, Piscataway, NJ). Processed blots were scanned in a Typhoon 9410 scanner (Amersham Biosciences). Results shown are representative of three separate experiments.

(0.05–0.25 unit pH increase). This was a similar but less pronounced effect than that previously seen by Liu et al. (increase of 0.5 unit from pH 4.5 to 5.0) in chronic exposure of less mature (1–2 weeks post-confluence) ARPE-19 cells to moderate levels of A2E (14 nM, twice per week for 4 weeks) [21]. We suggest that maintaining ARPE-19 cells for longer post-confluence before experiments allows them to become more resistant to the lysosome-alkalinizing effect of A2E, perhaps due to greater differentiation. Alkalinization of lysosomes is well-known to lead to lysosomal function impairment but leads to induction of melanogenesis in the melanosomes of melanocytes [59]. Agent H89, a pharmacological inhibitor of protein kinase A, which prevents alkalinization of melanosomes, also completely blocks melanin synthesis in melanocytes [59]. However, RPE melanosomes protect ARPE-19 cells from oxidative stress [38], and exogenous melanin/melanosomes protect A2E from photooxidation inside RPE cells [25]. Our results also suggest a protective effect on ARPE-19 lysosomes when pigment was induced by A2E. The detrimental effect of micromolar amounts of A2E on retinal microglia was recently documented and coincided with increased microglial activation and decreased microglial neuroprotection of photoreceptors [60]. Although RPE cells might be able to compensate for low-level chronic A2E accumulation, retinal microglia could be more sensitive to A2E toxicity and thus may provide a cellular mechanism for the pathogenesis of age-related macular degeneration. Taking these observations together, we propose that A2E-induced alkalinization of lysosomes could serve a physiologic role in maintaining melanin pigmentation of RPE cells. This is consistent with observations in melanocytes that the pH optimum of TYR is at 7.4 [61] and that the later steps in eumelanogenesis after dopachrome are also optimal at neutral pH [62]. It is also consistent with pathophysiological findings in *Abca4* null mice in which melanin-related 790 nm autofluorescence increased in parallel with A2E-related 488 nm autofluorescence from 1 to 6 months of age [63]. In future studies, we plan to dissect the molecular mechanisms involved in these fundamental aspects of RPE biology.

APPENDIX 1. STR GENOTYPE AND AMELOGENIN GENDER-DETERMINING LOCUS OF ARPE-19 CELL BATCH USED.

To access the data, click or select the words "Appendix 1."

APPENDIX 2. UPTAKE OF A2E BY ARPE-19 CELLS.

Uptake of A2E in the 100 nM-10 µM range was linear in both single and multiple treatment experiments. Data was calculated from area under the curve of A2E peaks detected at 430 nm in reversed phase HPLC analyses of extracts of cells single-fed or multiple-fed 10 µM, 1 µM and 100 nM A2E delivered in DMSO. To access the data, click or select the words "Appendix 2."

APPENDIX 3. MASS SPECTROMETRIC ANALYSIS OF MELANIN.

Acetonitrile extracts of lysosomal fractions and synthetic melanin were analyzed using MALDI-TOF mass spectrometry. **A**: Lysosomal fractions isolated from multiple 1 µM A2E-treated ARPE-19 cells; **B**: Synthetic melanin standard. M/z peaks of 441, 495, 523, 537, 551, 565 were common between ARPE-19 lysosomal extracts and synthetic melanin spectra (see inset box in panel B for expansion of synthetic melanin masses between m/z 405 and 602), but the lower m/z peaks of 304, 329 and 332 found in synthetic melanin were not. Results shown are representative of three separate experiments. To access the data, click or select the words "Appendix 3."

APPENDIX 4. APPARENT CO-LOCALIZATION OF A2E AND MELANIN IN ARPE-19 LYSOSOMAL FRACTIONS.

UV-Vis spectra (range 300–720 nm) of lysosomal fractions 1–5 isolated from multiple 1 µM A2E-treated cells showing co-localization of A2E (λ_{max}=439 nm) and melanin (λ_{max}=335 nm) in fractions 3 and 4. To access the data, click or select the words "Appendix 4."

ACKNOWLEDGMENTS

This research was supported by the Intramural Research Program of the National Eye Institute, and of the National Center for Advancing Translational Sciences, National Institutes of Health. T.P. was supported by the Howard Hughes Medical Institute. We thank Dr. Robert N. Fariss and Dr. Maria M. Campos, Biological Imaging Core, NEI for assisting with confocal microscopy.

REFERENCES

1. Sparrow JR, Wu Y, Kim CY, Zhou J. Phospholipid meets all-trans-retinal: the making of RPE bisretinoids. J Lipid Res 2010; 51:247-61. [PMID: 19666736].

2. Boyer NP, Higbee D, Currin MB, Blakeley LR, Chen C, Ablonczy Z, Crouch RK, Koutalos Y. Lipofuscin and N-retinylidene-N-retinylethanolamine (A2E) accumulate in retinal pigment epithelium in absence of light exposure: their origin is 11-cis-retinal. J Biol Chem 2012; 287:22276-86. [PMID: 22570475].

3. Kim SR, He J, Yanase E, Jang YP, Berova N, Sparrow JR, Nakanishi K. Characterization of dihydro-A2PE: an intermediate in the A2E biosynthetic pathway. Biochemistry 2007; 46:10122-9. [PMID: 17685561].

4. Bakall B, Radu RA, Stanton JB, Burke JM, McKay BS, Wadelius C, Mullins RF, Stone EM, Travis GH, Marmorstein AD. Enhanced accumulation of A2E in individuals homozygous or heterozygous for mutations in BEST1 (VMD2). Exp Eye Res 2007; 85:34-43. [PMID: 17477921].

5. Mata NL, Weng J, Travis GH. Biosynthesis of a major lipofuscin fluorophore in mice and humans with ABCR-mediated retinal and macular degeneration. Proc Natl Acad Sci USA 2000; 97:7154-9. [PMID: 10852960].

6. Vasireddy V, Jablonski MM, Khan NW, Wang XF, Sahu P, Sparrow JR, Ayyagari R. Elovl4 5-bp deletion knock-in mouse model for Stargardt-like macular degeneration demonstrates accumulation of ELOVL4 and lipofuscin. Exp Eye Res 2009; 89:905-12. [PMID: 19682985].

7. Congdon N, O'Colmain B, Klaver CC, Klein R, Munoz B, Friedman DS, Kempen J, Taylor HR, Mitchell P. Causes and prevalence of visual impairment among adults in the United States. Arch Ophthalmol 2004; 122:477-85. [PMID: 15078664].

8. O'Shea JG. Age-related macular degeneration: a leading cause of blindness. Med J Aust 1996; 165:561-4. [PMID: 8941243].

9. Starr CE, Guyer DR, Yannuzzi LA. Age-related macular degeneration. Can we stem this worldwide public health crisis? Postgrad Med 1998; 103:153-6. [PMID: 9590992].

10. Cideciyan AV, Aleman TS, Swider M, Schwartz SB, Steinberg JD, Brucker AJ, Maguire AM, Bennett J, Stone EM, Jacobson SG. Mutations in ABCA4 result in accumulation of lipofuscin before slowing of the retinoid cycle: a reappraisal of the human disease sequence. Hum Mol Genet 2004; 13:525-34. [PMID: 14709597].

11. Kim SR, Fishkin N, Kong J, Nakanishi K, Allikmets R, Sparrow JR. Rpe65 Leu450Met variant is associated with reduced levels of the retinal pigment epithelium lipofuscin fluorophores A2E and iso-A2E. Proc Natl Acad Sci USA 2004; 101:11668-72. [PMID: 15277666].

12. Weng J, Mata NL, Azarian SM, Tzekov RT, Birch DG, Travis GH. Insights into the function of Rim protein in photoreceptors and etiology of Stargardt's disease from the phenotype in abcr knockout mice. Cell 1999; 98:13-23. [PMID: 10412977].

13. Pawar AS, Qtaishat NM, Little DM, Pepperberg DR. Recovery of rod photoresponses in ABCR-deficient mice. Invest Ophthalmol Vis Sci 2008; 49:2743-55. [PMID: 18263807].

14. Blakeley LR, Chen C, Chen CK, Chen J, Crouch RK, Travis GH, Koutalos Y. Rod outer segment retinol formation is independent of Abca4, arrestin, rhodopsin kinase, and rhodopsin palmitylation. Invest Ophthalmol Vis Sci 2011; 52:3483-91. [PMID: 21398289].

15. Sparrow JR, Parish CA, Hashimoto M, Nakanishi K. A2E, a lipofuscin fluorophore, in human retinal pigmented epithelial cells in culture. Invest Ophthalmol Vis Sci 1999; 40:2988-95. [PMID: 10549662].

16. Finnemann SC, Leung LW, Rodriguez-Boulan E. The lipofuscin component A2E selectively inhibits phagolysosomal degradation of photoreceptor phospholipid by the retinal pigment epithelium. Proc Natl Acad Sci USA 2002; 99:3842-7. [PMID: 11904436].

17. Bergmann M, Schutt F, Holz FG, Kopitz J. Inhibition of the ATP-driven proton pump in RPE lysosomes by the major lipofuscin fluorophore A2-E may contribute to the pathogenesis of age-related macular degeneration. FASEB J 2004; 18:562-4. [PMID: 14715704].

18. Sparrow JR, Nakanishi K, Parish CA. The lipofuscin fluorophore A2E mediates blue light-induced damage to retinal pigmented epithelial cells. Invest Ophthalmol Vis Sci 2000; 41:1981-9. [PMID: 10845625].

19. Schutt F, Bergmann M, Holz FG, Kopitz J. Isolation of intact lysosomes from human RPE cells and effects of A2-E on the integrity of the lysosomal and other cellular membranes. Graefe's archive for clinical and experimental ophthalmology = Albrecht Von Graefes Arch Klin Exp Ophthalmol 2002; 240:983-8. .

20. Holz FG, Schutt F, Kopitz J, Eldred GE, Kruse FE, Volcker HE, Cantz M. Inhibition of lysosomal degradative functions in RPE cells by a retinoid component of lipofuscin. Invest Ophthalmol Vis Sci 1999; 40:737-43. [PMID: 10067978].

21. Liu J, Lu W, Reigada D, Nguyen J, Laties AM, Mitchell CH. Restoration of lysosomal pH in RPE cells from cultured human and ABCA4(−/−) mice: pharmacologic approaches and functional recovery. Invest Ophthalmol Vis Sci 2008; 49:772-80. [PMID: 18235027].

22. Vives-Bauza C, Anand M, Shirazi AK, Magrane J, Gao J, Vollmer-Snarr HR, Manfredi G, Finnemann SC. The age lipid A2E and mitochondrial dysfunction synergistically impair phagocytosis by retinal pigment epithelial cells. J Biol Chem 2008; 283:24770-80. [PMID: 18621729].

23. Ablonczy Z, Higbee D, Anderson DM, Dahrouj M, Grey AC, Gutierrez D, Koutalos Y, Schey KL, Hanneken A, Crouch RK. Lack of correlation between the spatial distribution of A2E and lipofuscin fluorescence in the human retinal pigment epithelium. Invest Ophthalmol Vis Sci 2013; 54:5535-42. [PMID: 23847313].

24. Ablonczy Z, Higbee D, Grey AC, Koutalos Y, Schey KL, Crouch RK. Similar molecules spatially correlate with lipofuscin and N-retinylidene-N-retinylethanolamine in the mouse but not in the human retinal pigment epithelium. Arch Biochem Biophys 2013; 539:196-202. [PMID: 23969078].

25. Wang Z, Dillon J, Gaillard ER. Antioxidant properties of melanin in retinal pigment epithelial cells. Photochem Photobiol 2006; 82:474-9. [PMID: 16613501].

26. Rózanowski B, Burke JM, Boulton ME, Sarna T, Rozanowska M. Human RPE melanosomes protect from photosensitized and iron-mediated oxidation but become pro-oxidant in the presence of iron upon photodegradation. Invest Ophthalmol Vis Sci 2008; 49:2838-47. [PMID: 18326697].

27. Parish CA, Hashimoto M, Nakanishi K, Dillon J, Sparrow J. Isolation and one-step preparation of A2E and iso-A2E, fluorophores from human retinal pigment epithelium. Proc Natl Acad Sci USA 1998; 95:14609-13. [PMID: 9843937].

28. Papermaster DS, Dreyer WJ. Rhodopsin content in the outer segment membranes of bovine and frog retinal rods. Biochemistry 1974; 13:2438-44. [PMID: 4545509].

29. Schertler GF, Hargrave PA. Preparation and analysis of two-dimensional crystals of rhodopsin. Methods Enzymol 2000; 315:91-107. [PMID: 10736696].

30. Strunnikova N, Zhang C, Teichberg D, Cousins SW, Baffi J, Becker KG, Csaky KG. Survival of retinal pigment epithelium after exposure to prolonged oxidative injury: a detailed gene expression and cellular analysis. Invest Ophthalmol Vis Sci 2004; 45:3767-77. [PMID: 15452088].

31. Kollias N. The spectroscopy of human melanin pigmentation. In: Zeise L, editor. Melanin:Its role in human photoprotection: Valdenmar publishing co; 1995. p. 31–8.

32. Jang YP, Matsuda H, Itagaki Y, Nakanishi K, Sparrow JR. Characterization of peroxy-A2E and furan-A2E photooxidation products and detection in human and mouse retinal pigment epithelial cell lipofuscin. J Biol Chem 2005; 280:39732-9. [PMID: 16186115].

33. Krogstad DJ, Schlesinger PH, Gluzman IY. Antimalarials increase vesicle pH in Plasmodium falciparum. J Cell Biol 1985; 101:2302-9. [PMID: 3905824].

34. Bowman EJ, Siebers A, Altendorf K. Bafilomycins: a class of inhibitors of membrane ATPases from microorganisms, animal cells, and plant cells. Proc Natl Acad Sci USA 1988; 85:7972-6. [PMID: 2973058].

35. Christensen KA, Myers JT, Swanson JA. pH-dependent regulation of lysosomal calcium in macrophages. J Cell Sci 2002; 115:599-607. [PMID: 11861766].

36. Ohkuma S, Poole B. Fluorescence probe measurement of the intralysosomal pH in living cells and the perturbation of pH by various agents. Proc Natl Acad Sci USA 1978; 75:3327-31. [PMID: 28524].

37. Coffey JW, De Duve C. Digestive activity of lysosomes. I. The digestion of proteins by extracts of rat liver lysosomes. J Biol Chem 1968; 243:3255-63. [PMID: 5656369].

38. Burke JM, Kaczara P, Skumatz CM, Zareba M, Raciti MW, Sarna T. Dynamic analyses reveal cytoprotection by RPE melanosomes against non-photic stress. Mol Vis 2011; 17:2864-77. [PMID: 22128234].

39. Sundelin SP, Nilsson SE, Brunk UT. Lipofuscin-formation in cultured retinal pigment epithelial cells is related to their melanin content. Free Radic Biol Med 2001; 30:74-81. [PMID: 11134897].

40. Pezzella ANA, d'Ischia M, Prota G, Seraglia R, Traldi P. Identification of partially degraded oligomers of 5,6-Dihydroindole-2-carboxylic acid in Sepia melanin by matrix-assisted laser desorption/ionization mass spectrometry. Rapid Commun Mass Spectrom 1997; 11:368-72. .

41. Roth F, Bindewald A, Holz FG. Keypathophysiologic pathways in age-related macular disease. Graefes Arch Clin Exp Ophthalmol 2004; 242:710-6. [PMID: 15309554].

42. Bindewald A, Schmitz-Valckenberg S, Jorzik JJ, Dolar-Szczasny J, Sieber H, Keilhauer C, Weinberger AW, Dithmar S, Pauleikhoff D, Mansmann U, Wolf S, Holz FG. Classification of abnormal fundus autofluorescence patterns in the junctional zone of geographic atrophy in patients with age related macular degeneration. Br J Ophthalmol 2005; 89:874-8. [PMID: 15965170].

43. Sparrow JR, Yoon KD, Wu Y, Yamamoto K. Interpretations of fundus autofluorescence from studies of the bisretinoids of the retina. Invest Ophthalmol Vis Sci 2010; 51:4351-7. [PMID: 20805567].

44. Rudolf M, Vogt SD, Curcio CA, Huisingh C, McGwin G Jr, Wagner A, Grisanti S, Read RW. Histologic basis of variations in retinal pigment epithelium autofluorescence in eyes with geographic atrophy. Ophthalmology 2013; 120:821-8. [PMID: 23357621].

45. Greenberg JP, Duncker T, Woods RL, Smith RT, Sparrow JR, Delori FC. Quantitative fundus autofluorescence in healthy eyes. Invest Ophthalmol Vis Sci 2013; 54:5684-93. [PMID: 23860757].

46. Lakkaraju A, Finnemann SC, Rodriguez-Boulan E. The lipofuscin fluorophore A2E perturbs cholesterol metabolism in retinal pigment epithelial cells. Proc Natl Acad Sci USA 2007; 104:11026-31. [PMID: 17578916].

47. Radu RA, Mata NL, Nusinowitz S, Liu X, Sieving PA, Travis GH. Treatment with isotretinoin inhibits lipofuscin accumulation in a mouse model of recessive Stargardt's macular degeneration. Proc Natl Acad Sci USA 2003; 100:4742-7. [PMID: 12671074].

48. Roberts JE, Kukielczak BM, Hu DN, Miller DS, Bilski P, Sik RH, Motten AG, Chignell CF. The role of A2E in prevention or enhancement of light damage in human retinal pigment epithelial cells. Photochem Photobiol 2002; 75:184-90. [PMID: 11883606].

49. Suter M, Reme C, Grimm C, Wenzel A, Jaattela M, Esser P, Kociok N, Leist M, Richter C. Age-related macular degeneration. The lipofusion component N-retinyl-N-retinylidene ethanolamine detaches proapoptotic proteins from mitochondria and induces apoptosis in mammalian retinal pigment epithelial cells. J Biol Chem 2000; 275:39625-30. [PMID: 11006290].

50. Dayhaw-Barker P. Retinal pigment epithelium melanin and ocular toxicity. Int J Toxicol 2002; 21:451-4. Review[PMID: 12537641].

51. Feeney L. Lipofuscin and melanin of human retinal pigment epithelium. Fluorescence, enzyme cytochemical, and

ultrastructural studies. Invest Ophthalmol Vis Sci 1978; 17:583-600. [PMID: 669890].

52. Raposo G, Tenza D, Murphy DM, Berson JF, Marks MS. Distinct protein sorting and localization to premelanosomes, melanosomes, and lysosomes in pigmented melanocytic cells. J Cell Biol 2001; 152:809-24. [PMID: 11266471].

53. Hellström AR, Watt B, Fard SS, Tenza D, Mannstrom P, Narfstrom K, Ekesten B, Ito S, Wakamatsu K, Larsson J, Ulfendahl M, Kullander K, Raposo G, Kerje S, Hallbook F, Marks MS, Andersson L. Inactivation of Pmel alters melanosome shape but has only a subtle effect on visible pigmentation. PLoS Genet 2011; 7:e1002285-[PMID: 21949658].

54. Dell'Angelica EC, Mullins C, Caplan S, Bonifacino JS. Lysosome-related organelles. FASEB J 2000; 14:1265-78. [PMID: 10877819].

55. Diment S, Eidelman M, Rodriguez GM, Orlow SJ. Lysosomal hydrolases are present in melanosomes and are elevated in melanizing cells. J Biol Chem 1995; 270:4213-5. [PMID: 7876179].

56. Schraermeyer U, Heimann K. Current understanding on the role of retinal pigment epithelium and its pigmentation. Pigment Cell Res 1999; 12:219-36. [PMID: 10454290].

57. Schraermeyer U, Peters S, Thumann G, Kociok N, Heimann K. Melanin granules of retinal pigment epithelium are connected with the lysosomal degradation pathway. Exp Eye Res 1999; 68:237-45. [PMID: 10068489].

58. Damek-Poprawa M, Diemer T, Lopes VS, Lillo C, Harper DC, Marks MS, Wu Y, Sparrow JR, Rachel RA, Williams DS, Boesze-Battaglia K. Melanoregulin (MREG) modulates lysosome function in pigment epithelial cells. J Biol Chem 2009; 284:10877-89. [PMID: 19240024].

59. Cheli Y, Luciani F, Khaled M, Beuret L, Bille K, Gounon P, Ortonne JP, Bertolotto C, Ballotti R. {alpha}MSH and Cyclic AMP elevating agents control melanosome pH through a protein kinase A-independent mechanism. J Biol Chem 2009; 284:18699-706. [PMID: 19389708].

60. Ma W, Coon S, Zhao L, Fariss RN, Wong WT. A2E accumulation influences retinal microglial activation and complement regulation. Neurobiol Aging 2013; 34:943-60. [PMID: 22819137].

61. Fuller BB, Spaulding DT, Smith DR. Regulation of the catalytic activity of preexisting tyrosinase in black and Caucasian human melanocyte cell cultures. Exp Cell Res 2001; 262:197-208. [PMID: 11139343].

62. Ito S, Suzuki N, Takebayashi S, Commo S, Wakamatsu K. Neutral pH and copper ions promote eumelanogenesis after the dopachrome stage. Pigment Cell Melanoma Res. 2013; 26:817-25. [PMID: 23844795].

63. Charbel Issa P, Barnard AR, Singh MS, Carter E, Jiang Z, Radu RA, Schraermeyer U, Maclaren RE. Fundus Autofluorescence in the Abca4−/− Mouse Model of Stargardt Disease–Correlation With Accumulation of A2E, Retinal Function, and Histology. Invest Ophthalmol Vis Sci 2013; 54:5602-12. [PMID: 23761084].

Articles are provided courtesy of Emory University and the Zhongshan Ophthalmic Center, Sun Yat-sen University, P.R. China. The print version of this article was created on 14 March 2014. This reflects all typographical corrections and errata to the article through that date. Details of any changes may be found in the online version of the article.